Optical Biopsy

Irving J. Bigio
Boston University, Boston, Massachusetts, U.S.A.

Judith R. Mourant
Los Alamos National Laboratory, Los Alamos, New Mexico, U.S.A.

INTRODUCTION

This article reviews the application of various types of optical spectroscopy and metrology to minimally invasive medical diagnostics. The promises and hopes, as well as the difficulties, of these developing techniques are discussed.

The term ''optical biopsy'' has entered into common usage among researchers in the field of biomedical optics. Although it is inherently an inaccurate term—it is perhaps something of an oxymoron because ''biopsy'' refers specifically to the removal of tissue, whereas the implication of ''optical'' is that tissue is not removed—it is nonetheless commonly understood to represent the use of some form of optical measurement, often a type of spectroscopy, to noninvasively (or minimally invasively) perform a tissue diagnosis, in situ, in vivo, and in real-time. The motivation is to reduce the need for surgical removal of biopsy tissue samples; rather, some form of spectral analysis of the tissue is recorded in vivo by an imaging system or with an optical probe placed on or near the surface of the tissue in question. The measurement is frequently mediated by optical fibers, and a diagnosis of the tissue is then attempted based on the optical measurements.

For a number of endoscopic applications, for which ''random'' biopsies are often taken in an attempt to find premalignant or early malignant conditions, an instant optical measurement could enable ''guided biopsy,'' with increased probability for sampling a diseased site, while reducing the number of tissue samples. Thus, additional motivation is provided by the potential for reduced healthcare costs as a consequence of eliminating unnecessary histology. Moreover, the immediacy of diagnostic information can reduce the emotional trauma to the patient awaiting an answer. For diseases of the gastrointestinal (GI) tract, for example, the potential benefits of optical tissue diagnosis can be significant. Several disorders of the GI tract are correlated with a predisposition for cancer, including colitis, colon polyps, and Barrett's esophagus. Typically, these diseases are followed with annual (or more frequent) endoscopic examination accompanied by tissue biopsies. As many as 20–30 ''random'' biopsies may be taken in one session. This is a time-consuming (and therefore expensive) procedure, which entails some degree of risk for the patient. For each conventional biopsy, the biopsy tool must be withdrawn from the endoscope and the specimen removed before the tool can be reinserted for the next biopsy. In contrast, an optical diagnostic probe could be moved from site to site in succession, with each measurement being recorded in a fraction of a second, by simply moving the location of the probe tip. When a diseased site is found, the surgical biopsy can be performed at that particular site.

OVERVIEW

Obviously there are also potential applications for optical biopsy that do not require endoscopes. Skin cancers and cervical cancer are immediate examples. Moreover, optical biopsy can also serve as an aid in various surgical procedures by, for example, helping to identify tumor margins in real-time. In summary, optical diagnostic techniques offer the potential to improve disease management, with reduced risks for the patient, and with the potential for earlier diagnosis and immediate treatment.

Optical methods have also been the subject of intense research aimed at developing noninvasive monitors for glucose and other blood analytes. Such applications deviate from the implication of optical biopsy and might be better classified under optical sensors or noninvasive blood chemistry. Consequently, they are not treated in this chapter.

A range of spectroscopies have been investigated for optical diagnosis, all of which have one basic principle in common. The specific optical spectrum of a tissue sample contains information about the biochemical composition and/or the structure of the tissue. Biochemical information can be obtained by measuring absorption, fluorescence, or Raman scattering signals. Structural and morphological information may be obtained by techniques that look at

Encyclopedia of Optical Engineering
DOI: 10.1081/E-EOE 120009717

MARCEL DEKKER, INC.
270 Madison Avenue, New York, New York 10016

the elastic-scattering properties of tissue. These basic approaches are useful for the detection of cancer as well as for other diagnostic applications such as blood oxygen saturation, intraluminal detection of atherosclerosis, and simply the identification of different tissue types during surgical procedures.

Some research groups have been attempting to develop intraluminal (sometimes fiber optic-mediated) approaches to optical coherence tomography or confocal microscopy, as methods of performing microscopic imaging of subsurface cellular structure, in situ. These methods might likewise be logically included under the umbrella term ''optical biopsy.'' However, the technical approaches to those methods, and the intent of the technologies, are sufficiently different that they are covered under a different chapter of this Encyclopedia.

FLUORESCENCE SPECTROSCOPY

Tissues may contain several fluorescent chromophores (fluorophores) such as NADH, elastin, collagen, and flavins. By spectrally measuring the ultraviolet (UV)-induced fluorescence of tissue, it should, in principle, be possible to learn about the relative concentrations and redox states of such compounds, and by extension to learn something about the biochemical state of the tissue. In other words, a motivation for utilizing fluorescence spectroscopy for the diagnosis of tissue pathologies is that fluorescence is sensitive to changes in the biochemical make-up of the tissue, which in turn reflects upon its pathology. However, several complications arise that make the fluorescence measurements in tissue significantly more complicated than a laboratory measurement of various fluorophores. Scattering cross-sections are quite high in tissue and depend on wavelength,[1] which can result in a distortion of the fluorescence spectrum. In various optical configurations used for measuring fluorescence, the scattering in tissue can cause apparent changes in the spectral shape of detected fluorescence. Tissue also contains nonfluorescent chromophores, such as hemoglobin. Absorption by such chromophores of the emitted light from fluorophores can result in artificial dips and peaks in the fluorescence spectra. Despite these difficulties, many studies invoking a variety of methods have shown that fluorescence spectroscopy can be used for optical tissue diagnosis, and methods are being developed to extract intrinsic fluorescence from measurements of turbid media.[2–6] Papazoglou has written an overview of the diagnosis of malignancies and atherosclerotic plaque using laser-induced fluorescence spectroscopy (LIFS).[7] Andersson-Engels et al.[8] have published a review on the subject of the in vivo use of fluorescence imaging, based on the fluorescence from both endogenous and exogenous fluorophores, and Ramanujam[9] has reviewed steady-state and time-resolved fluorescence on neoplastic and nonneoplastic model systems.

There are two issues that must be addressed when classifying the methodologies of LIFS: one is the possible administration of a fluorescent tumor marker, and the other is the question of whether the detection is a point measurement or a fluorescence image of an area of tissue surface. LIFS can detect the native tissue fluorescence resulting from naturally occurring (endogenous) fluorophores, and can also be used to detect emission from externally administered (exogenous) fluorescent drugs that concentrate preferentially in malignant or premalignant tissues. The fluorescence from such drugs provides a large signal, which can be helpful in the detection process[10,11] and may be used as a detection tool for imaging of the patterns of malignancy in a given area of tissue.[12] The use of a fluorescent tumor marker, however, is not an ideal solution for routine screening because the administration of an exogenous drug is essentially an invasive process and can result in concomitant undesirable side affects. Consequently, Food and Drug Administration (FDA) approval is required for the use of a photosensitizer, following extensive testing for safety and efficacy. When LIFS (usually with UV excitation) is used to detect intrinsic tissue fluorescence, or autofluorescence, as the diagnostic marker,[13–16] it becomes essentially noninvasive, although care must be taken to minimize the total UV exposure, especially to internal tissues.

Regarding the issue of whether single-point or imaging measurements are performed, if a small fiber-optic probe is used, then the fluorescence is measured at a single tissue site; whereas if filtered, video imaging technology is employed, then the result is spectrally selective image of a larger tissue surface. Typically, in a point measurement, the entire fluorescence spectrum is recorded for a given excitation wavelength, and this can be repeated quickly for additional excitation wavelengths. On the other hand, when the tissue surface is imaged, only a small number of combinations of illumination and emission wavelengths are recorded. Then these can be compared pixel-by-pixel for the entire image. Sometimes, several discrete emission wavelengths are recorded for a single excitation wavelength. Such multispectral imaging can be performed in a reasonably short time.[17,18] Hyperspectral imaging, in which a full spectrum is recorded for each pixel, is possible, and is a result of adaptations of technology previously developed for satellite-based surveillance. However, the time required for recording hyperspectral imaging data becomes an impediment for clinical application.

In short, point measurements provide a lot of spectroscopic information about one localized tissue site;

Marcel Dekker, Inc.
270 Madison Avenue, New York, New York 10016

whereas spectral imaging provides a modest amount of spectral information, but for a significant area of tissue surface.

Most point measurements of fluorescence make use of intrinsic fluorescence. However, some spectrally resolved measurements of exogenous fluorophores have been made,[19] and in some cases a combined measurement of fluorescence from exogenous and endogenous fluorophores has been used as a diagnostic tool. This combined approach, sometimes called ''contrast enhancement,'' has been adapted by Anderson-Engels et al.[20,21] and Svanberg et al.,[12] who made in vivo measurements of skin and multiple in vitro measurements of the prostate and breast tissue and in vivo measurements in the brain and lung.

Some of the earliest works on diagnostic fluorescence spectroscopy by Profio et al.[22] and by Alfano et al.[23] addressed differences in the native UV-induced fluorescence in tissues of different pathology states. Initial (in vitro) studies of autofluorescence as a consequence of a single excitation wavelength such as these have been performed on a wide variety of tissue types, including gynecological, kidney, lung, thymus, dental, and a variety of tissues in the GI tract.[20,24–30] In several of these studies, there is a general trend that fluorescence from normal tissue is greater than fluorescence from abnormal tissue. This trend and other correlations seen in in vitro studies have demonstrated the potential for fluorescence spectroscopy as a real-time, noninvasive diagnostic.

A more sophisticated method of autofluorescence diagnosis, called excitation–emission matrix spectroscopy, utilizes multiple-color illumination (sequentially), with the full fluorescence spectrum recorded for each excitation wavelength, and the data display typically looks like a contour map.[31] The different excitation wavelengths might be expected to variously excite different chromophores, resulting in more complex emission patterns with more information relevant to biochemical changes than for single-color excitation, and with presumed greater likelihood of distinguishing malignancy from normal conditions. This technique has been used for examining the fluorescence from brain tissue[32] and from skin in vivo,[33] and has been used in vitro both for identifying spectral regions of interest for diagnosing cervical cancer and oral neoplasia[34–36] and for distinguishing different organisms causing otitis media.[37] The general technique is based on earlier developments in the field of chemical engineering.[38,39]

While in vivo measurements can demonstrate a potential for diagnosing tissue pathologies, care must be taken in interpreting the results of in vitro measurements. The biochemical properties of tissue may be significantly different in vitro compared with in vivo. For example, the NAD^+/NADH ratio may change, and the blood content and oxidation state is likely to change. Both of these changes can influence fluorescence spectra in the UV and visible scales.[13,14,40] To truly test the effectiveness of noninvasive diagnostics, in vivo clinical trials must be performed with a significant number of patients. Clinical trials that include tens of patients have been performed for several organs including the colon, cervix, esophagus, and lung, and are described below. The criteria used for evaluation of the efficacy of these studies are sensitivity and specificity. Sensitivity is defined as the percentage of diseased sites that were found to be abnormal by the fluorescence diagnostic metric. Specificity is the percentage of normal sites that were found to be normal by the fluorescence diagnostic metric.

One clinical study of the applicability of fluorescence spectroscopy to the diagnosis of tissue pathologies of the esophagus included 48 patients.[16] A nitrogen-pumped dye laser at 410 nm was used for excitation via a fiber-optic probe. A period of about 5–10 sec was spent at each location to accurately locate the probe and record the data. Differential normalized fluorescence (DNF) signals were calculated by first dividing the intensity at each wavelength by the total area under the curve, and a baseline curve is calculated as the mean average of a selected number of normal samples. The DNF for a tissue sample is then the difference between its normalized fluorescence spectrum and the baseline curve. For the 104 tissue samples compared with histopathology results, the authors reported a sensitivity of 100% and a specificity of 98%. It should be noted that these numbers are for retrospective correlation, and not predictive diagnosis. Nonetheless, these figures are promising.

Another in vivo clinical trial has been performed to assess the efficacy of fluorescence spectroscopy for the diagnosis of pathologies of the cervix.[41,42] In this trial, 115 sites (66 colposcopically normal areas and 49 histologically abnormal areas) in 28 patients were examined. A nitrogen laser at 337 nm was used for illuminating the tissue. The fiber-optic probe, which has separate delivery and collection fibers, incorporated a tip with a 2-mm-thick quartz flat to maintain the same spacing between the fibers and the tissue for all measurements (in contrast to the fiber ends being in direct optical contact with the tissue, as in the trial described above). The diagnostic algorithm for spectroscopically separating normal from abnormal tissues compared a spectral feature (the normalized slope of the spectrum at 420–440 nm) with the relative peak fluorescence intensity, and was able to separate abnormal tissue with a sensitivity of 92% and a specificity of 90%. More specifically, cervical intraepithelial neoplasia (CIN) was diagnosed with a sensitivity of 87% and a specificity of 73%. Recently, fluorescence spectroscopy has been compared to colopscopy for

diagnosis of squamous interepithelial lesions and was found to yield improved results.[43]

A least three in vivo studies on the reliability of fluorescence spectroscopy for the diagnosis of colon cancer have been reported. In a study by Cothren et al., a nitrogen-pumped dye laser, at 370 nm, was used for excitation to examine 67 sites in 20 patients.[13] The probe used for light delivery and collection was similar to that used in the clinical study of cervical cancer described above. The metric in this case was quite simple—a plot of the intensity at 680 nm vs. the intensity at 460 nm. Using this diagnostic, a sensitivity of 100% and a specificity of 97% for detecting adenomas vs. normal and hyperplastic tissue was achieved. In a study by Schomaker et al., a nitrogen laser (337 nm) was used to examine 91 polyps and 86 normal colonic tissues in 61 patients.[15] In this study, the probe consisted of only one 600-μm optical fiber, which was used in contact with the tissue for both light delivery and light collection. After normalizing a fluorescence spectrum to unity, multivariate linear regression (MVLR) was used to determine which wavelengths were most significant for discrimination. In this manner, an algorithm for diagnosing neoplastic tissue with a specificity of 80% and a sensitivity of 92% was developed. When the MLVR analysis was performed on the polyps alone the sensitivities and specificities for separating neoplastic and nonneoplastic polyps were 86% and 77%, respectively. In a study of hyperplastic and adenomatous polyps, 351- and 364-nm excitation and emission in the spectral bandwidth range of 400–700 nm was imaged. A sensitivity of 83% for the identification of dysplastic polyps was achieved. All hyperplastic polyps were correctly identified.[44]

In the case of detection of severe dysplasia, fluorescence imaging is used as an adjunct to white-light endoscopy. A recent clinical trial of 65 patients demonstrated that with LIFS, the sensitivity and specificity for detection of severe dysplasia and cancer changed from 61.2% and 85.0%, respectively, to 89.8% and 78.4%, respectively.[45] In a literature study, the effectiveness of bronchoscopy alone to bronchoscopy plus laser-induced spectroscopy was compared. The detection rate for preinvasive lesions was found to increase from 40% to 80% when LIFS was added.[46]

The use of LIFS for the in vivo detection of skin pathologies has also been investigated, although the studies involved smaller numbers of patients/measurements. Skin contains the chromophores elastin, collagen, keratin, and NADH, which are expected to contribute to the fluorescence spectrum, as well as purely absorbing chromophores like melanin and hemoglobin. Leffell and Stetz studied the fluorescence of skin with 325-nm excitation in hopes of correlating the results with chronological or photoaging of the skin.[47] Although they did not notice any correlation with chronological aging, they did find a correlation with photoaging. This correlation is not believed to be caused by simple differences in melanin content, although this was not rigorously proven. Fluorescence from skin has also been considered as a diagnostic for skin cancer. Lohmann et al. have reported several studies of skin fluorescence for the diagnosis of melanoma.[48–50] In one study where 365-nm excitation was used on 147 lesions, they were able to distinguish benign nevi (''birthmarks'') from premalignant nevi and melanoma. The metric used was the ratio of the maximum fluorescence intensity outside the lesion to the maximum fluorescence intensity inside the lesion. This metric choice was motivated by the finding that the fluorescence intensity inside the tumor region was much smaller than normal tissue and the fluorescence intensity outside the tumor was larger than for normal tissue. However, few experimental details were provided. The results contradict the outcome observed by Sterenborg et al.,[51,52] who attempted to reproduce the results of Lohmann et al. and examined the fluorescence from several types of skin lesions, also with 365-nm excitation. They concluded that there was no significant differences between the fluorescence of control sites and nonmelanoma skin tumors. For the eight melanomas and eight benign pigmented lesions, they stated that ''Neither the shape of the fluorescence intensity distribution, nor the spatial distribution of the fluorescence intensity showed any signature specific to the histopathological nature of the lesions investigated.'' Also, by removing the stratum corneum and measuring the fluorescence, they established that an important component of the fluorescence is from keratin in the stratum granulosum. Minor contributions to the fluorescence from endogenous chromophores were also noted in the tumors, but were not reliable enough to be used as a cancer-diagnostic. Recently, delta-aminolevulinic acid has been investigated as a method for increasing the diagnostic potential of fluorescence.[53,54] Although the early imaging experiments show promise, no larger-scale clinical trials have been performed yet.

Another area of application for LIFS is the detection of atherosclerotic lesions. The microscopic pattern of fluorescence in atheromas was studied as early as 1956.[55] In the 1980s, researchers began investigating LIFS as an intraluminal diagnostic technique for arterial tissue[56,57] and developed optical-fiber catheters for in vivo use.[58] The diagnosis of arterial plaque is important for the application of laser angioplasty, and LIFS has been tested for guidance of laser ablation in vitro and in vivo.[7,59] Related to the detection of atherosclerotic plaque are investigations of LIFS for the identification of fibrotic endocardium and myocardium, and sinoatrial and atrioventricular nodal conduction tissue for the treatment of arrhythmia.[60,61] Also, work in the area of monitoring

heart electrical activity using voltage-sensitive dyes began in the early 1980s.[62,63]

This review does not cover the well-established uses of fluorescence in ophthalmology (e.g., retinal vessel imaging).[64] More recent research, however, has shown that LIFS, when applied to ocular tissues, may be useful in diagnosing both ocular and other pathologies. Zuclich et al. have studied the fluorescence of the human lens, with excitation–emission matrix spectroscopy, as a diagnostic for aging-related dysfunctions, and the predisposition for early onset of cataract formation.[65] Interesting correlations were found between spectral signatures and the age-appropriate condition of the lens. Fluorescence spectroscopy of the lens has also been shown to have potential for noninvasive diagnosis of diabetes mellitus.[66] Fluorescence spectroscopy may also be used for monitoring the metabolic state of the cornea.[67]

Measurements of NADH fluorescence have been used for monitoring metabolism, with some of the earliest work being reported by Chance and coworkers.[68] Renault et al. developed a system that combines fluorescence and reflectance for in situ on-line monitoring of NADH concentration in vivo.[69] More recently, NADH fluorescence has been applied to in vitro measurements of redox changes in ischemic myocutaneous flaps[70] and to measurement of metabolism in the heart and brain.[71,72] Beuthan et al. have also reported that the time-resolved fluorescence of NADH oscillates in vivo.[73]

Changes in the concentration of NADH or the redox state of flavin cofactors (e.g., FAD) are sometimes cited as the presumed origin of the fluorescence spectral signatures[74–76] that correlate with tissue pathologies such as cancer. Some authors have attempted to determine how changes in these and other chromophores affect the fluorescence signal. Ramanujam et al. fit in vivo fluorescence spectra to a model of turbid tissue fluorescence, which included contributions from NAD(P)H, FAD, collagen, and elastin, and took into account absorption by hemoglobin.[41] Although there is quite a bit of scatter in their data, they saw an average increase in NAD(P)H content and an average decrease in the contribution of collagen fluorescence as the tissue progresses from normal to CIN. In contrast, NAD(P)H fluorescence of colonic tissue measured in vitro appears to decrease as tissue progresses from normal to abnormal.[14] The increase in the contribution of collagen fluorescence seen by Ramanujam et al. for cervical tissue is related to the results of Schomaker et al. and Bottiroli et al., who assert that changes in fluorescence are at least partly attributable to differences in the structural organization of the tissue.[15,76] In particular, in the case of polyps, there is a thickening of the mucosa, which shields some of the underlying collagen fluorescence. Several studies to determine the underlying biochemical and tissue structural changes that cause a change in fluorescence of dysplastic tissue are underway. Brookner et al. have reported on the contribution of various biochemical and structural features to fluorescence from normal cervical tissue.[77]

ELASTIC-SCATTERING SPECTROSCOPY (ESS)

When ESS is employed for tissue diagnosis, the tissue pathologies are detected and diagnosed using spectral measurements of the elastic-scattered light, in a manner that is sensitive to both scattering and absorption properties of the tissue, over a wide range of wavelengths. The use of a technique that is sensitive to the wavelength dependence of scattering efficiency and angles, as well as to absorption bands, is based on the fact that many tissue pathologies, including a majority of cancer forms, exhibit significant architectural changes at the cellular and subcellular levels. The object in this approach is to generate spectral signatures of relevance to the tissue parameters that pathologists address. After preparing a slide, a pathologist performs a microscopic assessment (histopathology) of the cell architecture or morphology: the sizes and shapes of cells, the ratio of nuclear to cellular volume, the form of the bilipid membrane, clustering patterns, etc. Because the cellular components that cause elastic scattering have dimensions typically on the order of visible to near-infrared (IR) wavelengths, the elastic scattering properties will exhibit a wavelength dependence that is more complex compared to simple ($1/\lambda^4$) Rayeigh scattering. When source and detector fibers are sufficiently separated for the diffusion approximation to be valid (typically $\geq$0.5 cm), the spectral dependence of the collected light will be less sensitive to the size and shapes of the scattering centers. However, for small separations ($\leq$0.1 cm), as with an endoscope-compatible probe, the wavelength dependence is quite sensitive to details of the light scattering that depend on the shape and size of the scattering centers. Thus, for such geometries, morphology, and size, changes can be expected to cause significant changes in an optical signature that is derived from the wavelength dependence of elastic scattering. These principles underlying ESS have been discussed in publications by Bigio and Mourant et al.[78,79]

In clinical demonstrations of ESS for tissue diagnosis, probes are designed to be used in optical contact with the tissue under examination and have separate illuminating and collecting fibers (Fig. 1). Thus, the light that is collected and transmitted to the analyzing spectrometer must first undergo several scattering events through a small volume of the tissue before entering the collection fiber(s). No light is collected from surface reflection; therefore, ESS is probably a more accurate term for that

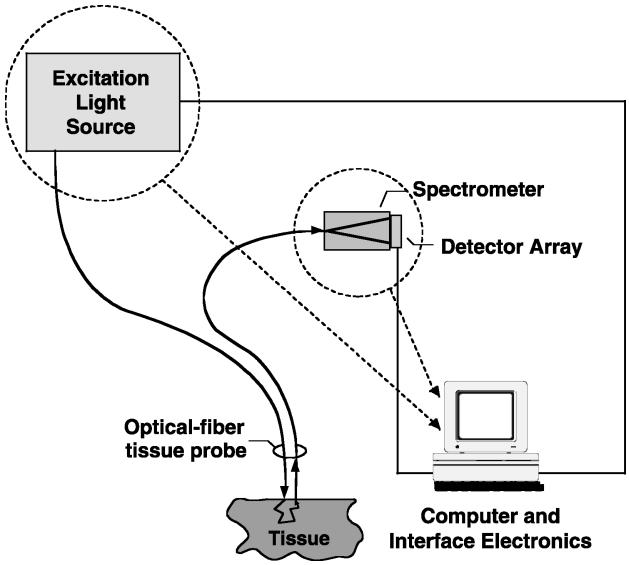

Fig. 1 Schematic diagram showing the optical geometry of the fiber-optic probe used in optical contact with the tissue for elastic-scattering spectroscopy. Only light that has multiply scattered through the tissue can enter the collection fiber.

method than ''reflectance'' spectroscopy. With the ESS geometry, the resulting effective path length of the collected photons is generally several times greater than the actual separation of the fiber tips. Consequently, in addition to the scattering spectral sensitivity to microscopic tissue morphology, this type of system can have good sensitivity to the optical absorption bands of the tissue components, over an effective operating range of 300 to >850 nm (with an adequately broad-bandwidth light source). Such absorption features add valuable complexity to the scattering spectral signature. It is important to note that the fiber probe, being used in optical contact with the tissue, examines only that site and does not image the tissue surface.

Although the type of instrument used generates a spectrum that characterizes the wavelength dependencies of both scattering and absorption of the tissue, without separating those contributions, these composite signatures appear to correlate well with differences in tissue types and condition. Mourant et al. have demonstrated the potential of this technique in vivo in the bladder, where a sensitivity and specificity of 100% and 97%, respectively, were obtained in preliminary clinical studies.[80] Koenig et al.[81] have also tested scattering spectroscopy for sensing bladder cancer, but with distributed illumination of the tissue. They observed the changes in hemoglobin absorption, as a result of increased perfusion in neoplastic areas, but did not sense the spectral differences associated with structural changes. Consequently, the sensitivity was good (91%) while the specificity was poor (60%) because simple inflammation can also cause increased perfusion.

Clinical tests of ESS for diagnosis of cancer in the GI tract have also shown encouraging results.[82,83] In an earlier study,[82] 60 sites in 16 patients were measured in the lower GI tract (colon and rectum). A spectral metric, based on the regions of the hemoglobin absorption bands (400–440 and 540–580 nm), was developed to separate the eight sites that were diagnosed under histopathology as being dysplasia (a potentially premalignant condition), adenoma (premalignant growth), or adenocarcinoma, from normal mucosa or more benign conditions (e.g., hyperplastic polyps or quiescent colitis). The sensitivity of this metric was 100% with a specificity of 98%, although this figure constitutes a retrospective correlation, not a predictive probability, and should be interpreted cautiously until measurements have been performed over a larger number of patients. A study with a larger database has been recently published by Ge et al.,[84] in which dysplastic and hyperplastic polyps of the colon were distinguished using the ESS method and neural-network pattern recognition for spectral classification. Zonios et al.[85] have also published a study applying ESS to diagnosis of colon polyps. In the study reported in Ref. [83], 67 biopsy sites were measured in 39 patients with Barrett's esophagus (a potentially premalignant growth of intestinal-type epithelium in the esophagus, resulting from chronic acid reflux). Diagnostic algorithms to distinguish dysplasia from nondysplastic Barrett's esophagus were developed using 80% of the data, and tested on the remaining 20%. (This was repeated five times, to cover all the available data, but the training and testing sets were always kept separate.) The resulting sensitivity and specificity were 82% and 80%, respectively. Wallace et al. have also recently studied Barrett's esophagus using a very similar ESS method, and likewise obtained encouraging results.[86]

Reflectance spectroscopy can be closely related to ESS, depending on the method of implementation. In general, we define reflectance spectroscopy as referring to the detection of both the diffuse and specular components of the reflectance, with a noncontact probe or with imaging optics. In some cases, measurements called ''reflectance'' or ''diffuse reflectance'' have been performed with contact probes, wherein the method is essentially identical to ESS.[69,85,87] Probes have been developed for sensing probe contact with the tissue and for making measurements at specified pressures.[88] These methods should reduce the variations in capillary perfusion resulting from variations in the pressure of the probe tip on the tissue surface.

The primary application of reflectance spectroscopy in the visible spectrum has been for studies of skin, and the optical properties of skin have been studied in some

Marcel Dekker, Inc.
270 Madison Avenue, New York, New York 10016

detail.[89,90] The use of the reflectance of light from skin as a diagnostic tool is an old technique—doctors have always derived information from visual observation of a patient. (A patient who appears blue may be hypoxic!) Dawson et al. developed a reflectance spectrometer and a theoretical model for indices of melanin and hemoglobin.[91] Feather et al. developed indices for hemoglobin and oxygenation,[92] and Hajizadeh-Saffar et al. have examined the accuracy of these indices.[93] Measurements of UV-induced pigmentation and erythema have also been made by Kollias and Baqer.[94] More recently, applications of reflectance spectrometry have also been developed for measurement of bilirubin concentration.[95,96]

The application of reflectance spectroscopy to the detection of skin cancer has been pursued by Marchesini et al. Their technique incorporates a modified integrating sphere with a standard UV/visible spectrophotometer, and measurements are made over the range 420–780 nm. In a study of 31 primary melanomas and 31 benign nevi, they were able distinguish the two groups with a sensitivity of 90.3% and a specificity of 77.4%.[97] They are now developing a charge-coupled device (CCD)-based imaging technique.[98] More recently, Wallace et al. have employed ESS, as specifically described above, for the detection of melanoma.[99]

Clinical studies have also addressed three applications of ESS to assist in diagnosis and management of breast cancer: a transdermal-needle diagnostic and two perioperative applications.[100] Instant diagnosis by ESS, with the same size needle as for fine-needle aspiration (FNA) cytology, would reduce patient anxiety (while waiting for a diagnosis) and, in some cases, permit immediate treatment. Image guidance for insertion of the needle, either manually or by robotic insertion, could provide the additional benefit of higher reliability (i.e., reduced false negatives) when compared with traditional FNA. Optical diagnosis also fits well with the general motivation of robotic biopsy because of the immediate diagnosis. For open surgery procedures, a potentially important purpose of ESS diagnosis is to provide a probe for the surgeon to use during wide local excision or partial mastectomy, for assessing the resection margins in real-time. This could reduce the number of required repeat surgeries, which follow the discovery of positive resection margins.[101] The third application being studied is the real-time assessment of the associated lymph nodes during surgery. Recent research has shown that if the sentinel (main) node draining a tumor area is removed and does *not* show cancer, then the chances of any other nodes in that region showing cancer are only 1%.[102] Thus if the sentinel node does not show cancer, the rest of the axillary (armpit area) nodes can be left in place, but if it does show cancer, then a full surgical axillary-node clearance must be performed. Using artificial intelligence pattern-recognition methods for spectral classification (neural networks and hierarchical cluster analysis), these studies have also yielded sensitivities and specificities in the 1980s.

Other areas of potential clinical benefit of the use of scattering spectroscopy for identifying tissues during surgery abound, and two recent publications have addressed applications in brain surgery. Johns et al.[103] investigated the use of scattering spectroscopy to distinguish gray matter from white matter, for use during procedures that invoke insertion of small probes into the brain for treatment of certain neurological disorders. Another study, conducted by Lin et al.,[104] compared fluorescence with scattering spectroscopy for assistance in brain tumor demarcation during surgery.

Polarization Effects in Elastic Scattering

The measurement of polarization properties of scattered light has the potential to provide more information than the measurement of unpolarized light scattering. The observation of interesting optical patterns generated by the propagation of polarized light in tissue has a long history. A cross-like figure was observed over the macular area when the eye was photographed using crossed polarizers as early as 1978.[105] Methods for obtaining effective scatterer size and concentration from polarized backscattering images of polystyrene spheres suspensions have been described[106] and the physical origin of pattern features is well understood.[107–111] Recently, a fiber-optic method for measuring polarized light scattering, which can be used to determine average scatterer size and density of polystyrene spheres, has been demonstrated.[107] Polarized fiber-optic and imaging measurements of cell suspensions also provide information about scattering structures.[112]

Polarization methods can also be used to reject some of the multiply scattered light from deep within the tissue of interest. The rejection of deeply penetrating light is important for the diagnosis of cancer because carcinomas typically originate in the epithelium, which constitutes the top few hundred microns of tissue. Jacques et al.[113] have presented polarization images of skin that display changes correlating with differences between benign pigmented nevi and freckles. The images are defined as $(I_{par} - I_{perp})/(I_{par} + I_{perp})$, where I_{par} is a measurement using parallel linear polarization for illumination and detection and I_{perp} uses perpendicular linear polarizers for illumination and detection. Their analysis demonstrates that such images provide information about the top few hundred microns of skin only. Polarized-light photography of skin has also been used to evaluate photoaging.[114] Recently, Backman et al. have taken a slightly different approach, using polarized light scattering to isolate light scattered from near the tissue

surface.[115] They make point measurements of I_{par} and I_{perp} and subtract the two intensities. The resulting spectrum is then fit to an expression derived from the Mie theory. They report that the distribution of cell-nucleus sizes obtained agrees with microscopic measurements. In a similar experiment, Sokolov et al. demonstrated that wavelength-dependent results were consistent with the scattering expected from epithelial cells.[116]

The basic physics of polarized light propagation in scattering media is still under active investigation. Yao and Wang have presented time-resolved movies of polarized light propagation in turbid media.[117] The preservation of polarization in lipid, myocardium, and polystyrene spheres has been studied in detail,[118,119] and methods for examining light scattered from tissues in the exact backscattering direction have also been developed.[120]

INFRARED (IR) AND RAMAN SPECTROSCOPIES

IR and Raman spectroscopic measurements can provide detailed molecular information about tissue. Consequently, these spectroscopies have the potential to generate important biochemical information for tissue diagnosis. Some of the medical applications of vibrational spectroscopy currently under investigation include characterization of atherosclerosis (plaque in arteries) and detection of cancer.

IR spectroscopy is the measurement of absorption at wavelengths between $\sim$5000 cm^{-1} (2000 nm) and 100 cm^{-1} (100,000 nm). At these wavelengths, most absorption arises from transitions between vibrational energy levels of the molecules being probed. A single biological molecule can have several absorbance bands because multiple vibrations can occur within a single molecule. The pattern of absorption bands depends strongly on the type(s) of molecules present and consequently IR spectroscopy is very sensitive to tissue biochemistry.

Raman spectroscopy is an inelastic scattering process, i.e. there is a difference between the energy of the incident and the scattered light. This scattering process causes either an increase (anti-Stokes) or a decrease (Stokes) in energy equal to the difference between two vibrational energy levels of the molecule scattering the light. The intensity of scattered light is typically plotted as a function of the energy difference between the incident and scattered light and this graph provides information on the molecular vibrations of the molecules.

Table 1 Major protein vibrations

Amide I	1600–1700 cm^{-1}
Amide II	1500–1600 cm^{-1}
CH_2 scissoring	$\sim$1450 cm^{-1}
CH_3 deformations and COO^- vibrations	$\sim$1400 cm^{-1}
Amide III	1200–1350 cm^{-1}

Table 2 Phospholipid vibrations

Symmetric methylene, $-CH_2-$, stretch	$\sim$2850 cm^{-1}
Asymmetric methylene, $-CH_2-$, stretch	$\sim$2920 cm^{-1}
C═O stretch	1710–1750 cm^{-1}
CH_2 scissoring	$\sim$1450 cm^{-1}
PO_2^- antisymmetric stretch	1220–1260 cm^{-1}
Symmetric PO_2^- stretch	1080–1090 cm^{-1}

Four major components of biological tissues that contribute to Raman and IR spectra are proteins (including collagen), lipids, nucleic acids, and water. Representative molecules of these classes are shown in Table 1. Proteins, phospholipids, and nucleic acids each possess their own unique spectra. The primary contributions of proteins to Raman and IR spectra are attributable to vibrations of the amide backbone.[121–124] Proteins also display a band near 1450 cm^{-1} attributable to CH_2 and CH_3 scissoring[125] and a band near 1400 cm^{-1} because of CH_3 deformations and vibrations of $COO-$.[126] Table 1 gives typical vibrational frequencies of globular proteins. In addition to globular proteins, carbohydrates also contribute to vibrational spectra of tissue. Glycogen (a large branched polymer of glucose residues) has vibrations in the 950–1500 cm^{-1} spectral region.[127] In measurements of cells containing high concentrations of glycogen, the glycogen bands at $\sim$1020, 1080, and 1150 cm^{-1} are easily discernable.[128]

Table 2 lists the major vibrations of phospholipids. These are vibrations primarily associated with stretches or deformations of CH_2, and PO_2^- groups.[129–131] Vibrations of C═O contribute to the carbonyl region of IR spectra.[129]

Several vibrations of nucleic acids are given in Table 3. Like phospholipids, the spectra of nucleic acids contain bands attributable to the vibrations of phosphate groups. Stretches caused by phosphodioxy, the PO_2^- group, and the phosphodiester O—P—O group are present.[125] Table 3 lists the strongest IR absorptions; the

Table 3 Nucleic acid vibrations

C═O stretch	1650–1720 cm^{-1}
Asymmetric PO_2^- (weak in Raman)	1220–1240 cm^{-1}
Symmetric PO_2^- stretch	$\sim$1100 cm^{-1}

Marcel Dekker, Inc.
270 Madison Avenue, New York, New York 10016

phosphodioxy backbone vibrations and the C═O stretching vibrations of the purine and pyrimidine bases. In the Raman spectra, the phosphodiester bands and additional vibrations of the bases have comparable Raman scattering intensity to the phosphodioxy vibrations.

The Fourier-transform IR spectra of some fibroblast cells are given in Fig. 2. Spectral features have been assigned based on the literature discussed above. Measurements were made in phosphate-buffered saline with the cells at a concentration of 10^8 cells/mL, and a pathlength of 100 μm.

Raman and IR spectroscopies both measure the vibrational spectra of molecules. Because the symmetry rules for the two processes can be different, the Raman and IR spectra for a given molecule can be subsequently different. As a general rule, IR spectroscopy is more useful for studying polar bonds (such as C═O and OH), while Raman spectroscopy is more sensitive to nonpolar groups (such as C═C and S—S). One of the most prominent examples of the difference between Raman and IR spectroscopies is the spectroscopy of water. Raman scattering of water is quite weak between about 900 and 3000 cm^{-1}, with the only distinct feature in this region being an H—O—H bend near 1620 cm^{-1}. Between 3000 and 3700 cm^{-1}, the Raman scattering resulting from an O—H stretch is quite strong. In contrast, water absorbs strongly in the IR from 1500 to 1750 cm^{-1}, with continued significant absorption below 1500 cm^{-1}. The intensity of IR light with a wavelength of 5 μm (2000 cm^{-1}) is reduced by a factor of 10 at a depth of only ~65 μm in pure water. At a wavelength of 6.1 μm (1640 cm^{-1}), water absorption is even stronger and the intensity is reduced by a factor of 10 at a depth of only 7 μm.[132] Therefore, the penetration of IR radiation is of limited value for in vivo measurements. In contrast, the visible and near-IR wavelengths used for Raman excitation penetrate deeply into tissue. For this reason primarily, Raman spectroscopy is the preferred vibrational technique for tissue characterization.

The application of Raman spectroscopy to tissue is challenging because it is a weak effect. Additionally, tissue fluorescence as well as Raman scattering and fluorescence from optical fibers complicate the measurement of Raman spectra of tissue in vivo. Initially, many of the measurements of biological systems were performed using 1064-nm excitation and FT–Raman instruments in order to avert tissue fluorescence. This method, however, was prohibitively slow with data acquisition times took as long as 30 min.[125] Recently, several technological developments have enabled the development of Raman systems using excitation in the 700- to 800-nm range with much greater throughput. These technical advancements include relatively inexpensive diode lasers, high-efficiency (80% throughput) holographic spectrographs, low-noise, high-efficiency (quantum efficiencies greater than 80%) CCD cameras, and holographic notch filters and dielectric filters with sharp cut-offs. The holographic notch filter is used to reject the excitation light from the collection path, while the dielectric filter is used to remove fiber (quartz) fluorescence and Raman scattering from the excitation path immediately before the sample. Recently, in vivo intravascular and GI measurements have been demonstrated by Buschman et al.[133] and Shim et al.[134] using incident laser powers of 100 mW and integration times of 30 and 5 sec, respectively. However, these systems have a minor disadvantage in that there is

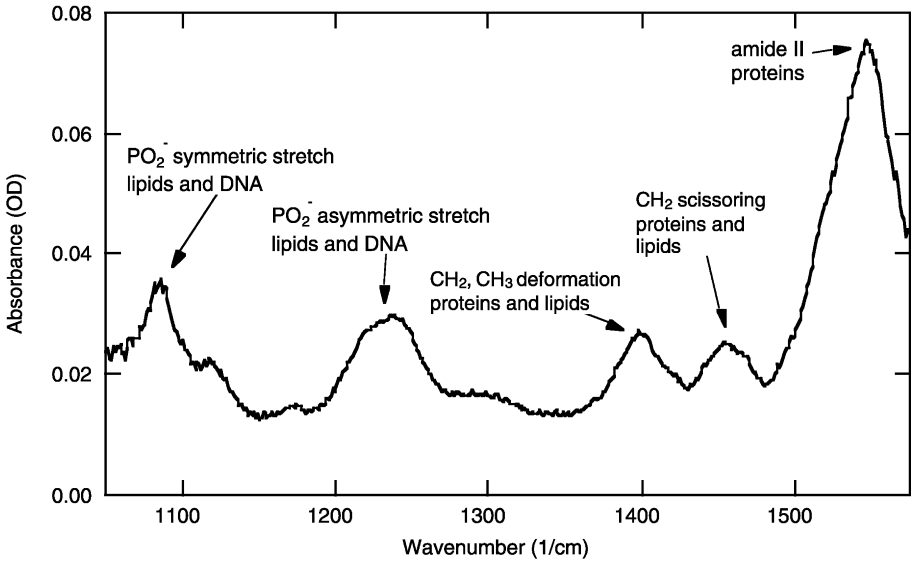

Fig. 2 IR spectra of fibroblast cells suspended in phosphate-buffered saline, obtained by Fourier transform spectroscopy.

some slowly varying fluorescence background that must be removed by subtraction of a low-order polynomial. Detectors with high efficiency and low-noise that could detect light at wavelengths longer than 1000 nm would alleviate this problem. However, more research is needed before such detectors become available.[135]

One final concern in the development of a Raman system with in vivo applications is that the intensity of light incident on the tissue must be limited to avoid tissue damage. Many of the current standards for skin exposure such as the American Conference of Governmental Industrial Hygienists (ACGIH) threshold limit values (TLVs) sometimes used by the FDA are quite low. The 2000 TLV for a 10-sec or greater skin exposure is 0.6 W/cm^2 at 900 nm. For a 400-μm delivery fiber, this only allows for an incident light power of 0.75 mW. Studies to establish less conservative values for tissue epithelial damage will be needed. At the red or near-IR wavelengths, the major concern is local heating of the tissue because near-IR light is nonmutagenic. Recently, tissue heating has been investigated experimentally. Experiments with an IR camera on ex vivo esophageal tissue show that 250 mW of 830-nm light focused to a spot size of 500 μm produces a temperature increase of less than 0.8° for an exposure time of 1 min.[134] These small thermal effects are not surprising because at wavelengths between 650 and ~1050 nm, light is only very weakly absorbed by tissue. Consequently, the incident light is spread out over a large volume because of scattering, and the temperature rise because of absorption at any particular location is quite small.

Two medical applications of Raman spectroscopy, that have been significantly investigated are the chemical assay of atherosclerotic plaque and diagnosis of cancers and precancerous lesions. In the case of atherosclerotic plaque, the goal is to be able to diagnosis the type of plaques that are most likely to rupture. The risk of rupture is largest in plaques with high levels extracellular cholesterol, low levels of collagen, and abundant macrophages.[133] The general goal of developing vibrational spectroscopy for cancer diagnosis is to develop a noninvasive method that can yield molecular information. The advantages of such methods are discussed in ''Introduction.''

In vitro IR experiments can help determine the potential of vibrational spectroscopy for assaying medically important changes in the molecular composition of tissue because the signal-to-noise ratio of IR measurements is higher than the corresponding Raman measurements. Numerous studies have been performed to determine whether IR spectroscopy is sensitive to carcinogenic/tumorigenic changes and these are summarized below. Furthermore, IR experiments can help in developing a link between biochemistry and spectroscopy. In vitro IR experiments can assist in the molecular assignments of spectral bands because of some vibrations that are not Raman-active are IR-active.

Nearly all of the in vitro studies have used fixed or frozen samples including the ones discussed below unless otherwise noted. Wong and coworkers have reported differences between cancerous and noncancerous tissue in several studies.[136–138] Malins and coworkers have noted a change in the spectra of DNA that is correlated with metastasis.[139,140] Detailed IR measurements have been performed on normal and leukemic lymphocytes.[141,142] The absorption at 1080 cm^{-1} divided by the absorption at 1540 cm^{-1} was found to be significantly different for 10 samples of B-chronic lymphatic leukemia and 10 normal samples. Furthermore, by comparing spectra of mixtures of ribonucleic acid (RNA)/deoxyribonucleic acid (DNA)/protein, DNA/protein, and RNA/protein to spectra of cells, it was found that the data are consistent with DNA/RNA ratios for normal lymphocytes reported in the literature. In a study of normal and malignant lung cancer cells similar to the study of lymphocytes described above, the absorption at 1080 cm^{-1} divided by the absorption at 1540 cm^{-1} was again found to be diagnostic.[143] The band at 1080 cm^{-1} is believed to be representative of nucleic acid content, while the 1540 cm^{-1} band is representative of protein content. Complete verification of these assignments has not been performed, however. As mentioned above, phospholipids could also contribute strongly to absorption at 1080 cm^{-1}. Multivariate analysis methods have been applied to the IR spectra of normal, hyperplastic, and neoplastic lymph cells.[144] A partial-least-squares classification method using spectral regions of 950–1725 and 2830–3000 cm^{-1} was able to distinguish hyperplastic and neoplastic tissue. The classification was performed using a cross-validation method; however, the normal spectra were not classified because of an insufficient number of samples. The contribution of glycogen to IR spectra of liver tissue has been studied. Vibrations of glycogen contribute significantly between 900 and 1100 cm^{-1}.[128] Finally, IR spectra of cells fixed with ethanol and dehydrated were found to be sensitive to cell cycle.[145] The absorptions because of nucleic acids were found to be stronger in cells which were in the process of duplicating their DNA than for cells containing only one copy of their DNA.

In addition to in vitro IR studies that investigated the potential of vibrational spectroscopy to differentiate normal, precancerous, and cancerous conditions, there have also been some in vitro Raman studies of cells and excised tissue. A review of much of this work before 1996 is provided by Mahadevan-Jansen and Richards-Kortum.[125] More recently, Yazdi et al. have demonstrated that the ratio of two resonance Raman bands, associated with nucleotides and protein, respectively, may be used to

Marcel Dekker, Inc.
270 Madison Avenue, New York, New York 10016

separate malignant and nonmalignant breast and cervical cells.[146] In addition, they found that a ratio of bands known to be sensitive to nucleotide stacking was correlated with malignant changes. This study is notable in the literature because the cells were measured in aqueous media and their viability was checked. Differences between normal and malignant hepatocytes have also been noted. Using HeNe excitation (632.8 nm), Hawi et al. found that bands at 1040 and 1083 cm^{-1} increased in intensity and a feature at 1241 cm^{-1} decreased in intensity for malignant hepatocytes as compared to normal liver cells.[147] The assignment of these spectral lines to specific biochemical features is difficult. As noted by the authors, the band at 1241 cm^{-1} could originate from either amide III vibrations or antisymmetric PO_2^- stretches of DNA. The results of this study should be treated with caution because the cells were air-dried. Dehydration is expected to affect the vibrational spectra. For example, spectral features of phospholipids are known to shift as a function of hydration.

Manohoran et al. measured the Raman spectra of 61 breast tissue samples.[148] Based on histopathological diagnosis, the specimens were grouped into normal (fat and glandular), benign (fibrocystic disease, adenosis), and malignant (carcinoma in situ and infiltrating ductal carcinoma). With knowledge of the pathology, the authors then used the results of a principal component analysis (PCA) in a logistic regression analysis to estimate the probability that a given sample belongs to one of the three diagnostic categories. They correctly classified 14 of 15 normal samples, 13 of 15 benign samples and all 31 malignant samples. Unfortunately, they did not have enough data to test their algorithm on an independent data set. A similar ex vivo study of cervical cancer has been performed.[149] Using PCA and Fisher's discriminant analysis, the authors were able to separate precancerous squamous intraepithelial lesions (SIL) from non-SIL with a sensitivity and specificity of 91% and 90%, respectively. Although these studies were performed on relatively small data sets, their results are encouraging.

Several in vitro Raman studies of arterial walls have been performed with the goal of developing Raman spectroscopy as a diagnostic methods for atherosclerotic plaque. The risk of rupture is higher when the plaque has large extracellular lipid and/or cholesterol deposits, and low concentrations of smooth muscle cells and collagen. Raman spectroscopy can quantify concentrations of cholesterol, phospholipid, and calcium salt.[150,151] Recently, it has been demonstrated that Raman spectroscopy can provide quantitative information about cholesterols and cholesteryl esters.[152]

The most amenable organ for an in vivo study is the skin. Consequently, most in vivo studies using Raman spectroscopy and all in vivo studies with IR spectroscopy have been performed on skin. Recently, in vivo IR absorption measurements of skin have been reported.[153] The measurements were performed using a silver-halide fiber with good IR transmission. The surface absorption was sensed with the evanescent wave using a fiber tissue contact length of a few millimeters. At 4 cm^{-1} resolution, recording times were about 15 sec and the tissue depth probed was estimated to be 20 μm. Spectral features such as amide I and amide II were noticeably different for skin on different parts of the body.

A Raman spectroscopic study has provided insight into the molecular composition of different skin layers, such as differences in concentrations of lipids and of natural moisturizing factor.[154] Another study has illustrated the complexity of measuring skin and the difficulties of unequivocal diagnosis by Raman spectroscopy.[155] Spectra are influenced by skin hydration, pigmentation, and nonmalignant abnormalities. More recently, Caspers et al. demonstrated that Raman spectra obtained in 5 sec can be used to determine the water concentration profiles in human skin.[156] The ability to carry out Raman measurements in the gastroentestinal tract has also been demonstrated very recently.[134] Spectra with good signal-to-noise ratio and a resolution of 12 cm^{-1} were obtained in 5 sec.

Finally, in vivo Raman spectroscopic measurements have been carried out on lamb and sheep arteries.[157] The measurements took 10–30 sec, each using 100 mW of 830-nm laser power at the tissue, and had a resolution of 10 cm^{-1}. The signal-to-noise ratio was sufficient to calculate weight percentages of calcium salts, cholesterol, protein, and phospholipids.

CONCLUSION

Optical spectroscopy for tissue diagnosis is being investigated for a wide range of clinical diagnostic needs, and metrics based on the spectral information are being developed for a wide variety of tissue pathologies. It is important to note that these metrics are likely to depend on the optical geometry of light delivery and collection. For example, with LIF the geometries used must be tailored to maximize the fluorescence collected from the regions of interest, which for epithelial cancers is near the surface of the tissue. The volume of tissue that is investigated by fiber-optic probes is being modeled by various groups.[158–161]

Each type of spectroscopy poses advantages and problems. While LIF has the advantage of being useful for surface imaging, it provides only rough information about tissue biochemistry. ESS, as defined here (distinguished from reflectance spectroscopy), is limited to point

measurements but it is sensitive to the cellular and subcellular structures that pathologists assess in histology (the ''gold'' standard). The use of less expensive detectors is enabled with ESS because the optical signals are much stronger than for LIF. Nonetheless, for both LIF and ESS, a white-light source (filtered in the case of LIF) can be employed rather than a laser, and the data acquisition and storage/display time of the best reported systems of both types is typically < 1 sec. Most of the developments of ESS and fluorescence spectroscopy discussed in this review have used unpolarized light. The use of polarized excitation and detection for both ESS and fluorescence may provide information for more detailed and/or accurate diagnosis of tissue pathology. Time-resolved broadband spectroscopy may also provide additional information in the case of LIF.

Raman and IR spectroscopies are the only methods that provide detailed information about the biomolecular constituents in the tissue. This type of detailed information can be essential for some diagnostic applications. In the case of IR spectroscopy, however, fiber-optic mediation is difficult, and only a very shallow depth of tissue can be assessed, often too shallow to be clinically useful. Raman spectroscopy, on the other hand, can probe appropriate volumes of tissue, but attaining adequate signal-to-noise ratio within a clinically acceptable integration time poses serious engineering (and fundamental) challenges.

In short, the potential benefits of optical biopsy methods in a variety of clinical applications are great enough that a broad range of research activities has emerged over the past decade at many major research institutions around the world, and the medical community has taken note of this trend.

REFERENCES

1. Cheong, W.; Prahl, S.A.; Welch, A.J. A review of the optical properties of biological tissues. IEEE J. Quantum Electron. **1990**, *26*, 2166–2185.
2. Durkin, A.J.; Jaikumar, S.; Ramanujam, N.; Richards-Kortum, R. Relation between fluorescence spectra of dilute and turbid samples. Appl. Opt. **1994**, *33*, 414–423.
3. Wu, J.; Feld, M.S.; Rava, R.P. Analytical model for extracting intrinsic fluorescence in turbid media. Appl. Opt. **1993**, *32*, 3585–3595.
4. Richards-Kortum, R.; Rava, R.P.; Cothren, R.; Metha, A.; Fitzmaurice, M.; Ratliff, N.B.; Kramers, J.R.; Kitrell, C.; Feld, M.S. A model for extraction of diagnostic information from laser induced fluorescence spectra of human artery wall. Spectrochim. Acta **1989**, *45A*, 87–93.
5. Richards-Kortum, R.; Rava, R.P.; Fitzmaurice, M.; Tong, L.L.; Ratliff, N.B.; Kramer, J.R.; Feld, M.S. A one-layer model of laser-induced fluorescence for diagnosis of disease in human tissue: Applications to atherosclerosis. IEEE Trans. Biomed. Eng. **1989**, *36*, 1222–1232.
6. Zhang, Q.G.; Muller, M.G.; Wu, J.; Feld, M.S. Turbidity-free fluorescence spectroscopy of biological tissue. Opt. Lett. **2000**, *25*, 1451–1453.
7. Papazoglou, T.G. Malignancies and atherosclerotic plaque diagnosis—is laser induced fluorescence spectroscopy the ultimate solution? J. Photochem. Photobiol., B Biol. **1995**, *28*, 3–11.
8. Andersson-Engels, S.; af Klinteberg, C.; Svanberg, K.; Svanberg, S. In vivo fluorescence imaging for tissue diagnostics. Phys. Med. Biol. **1997**, *42*, 815–824.
9. Ramanujam, N. Fluorescence spectroscopy of neoplastic and non-neoplastic tissues. Neoplasia **2000**, *2*, 89–117.
10. Profio, A.E., et al. Fluorescence Diagnosis of Cancer. In *Proc. of the Porphyrin Photosensitization Workshop, July, 1984*; Plenum Press, 1985; 43–50.
11. Kessel, D. Tumor localization and photosensitization by derivatives of hematoporphyrin: A review. IEEE J. Quantum Electron. **1987**, *23*, 1718–1720.
12. Svanberg, K., et al. Tissue characterization in some clinical specialties utilizing laser-induced fluorescence. Proc. SPIE **1994**, *2135*, 2–15.
13. Cothren, R.M.; Richards-Kortum, R.; Sivak, M.V.; Fitzmaurice, M.; Rava, R.P.; Boyce, G.A.; Doxtader, M.; Blackman, R.; Ivanc, T.B.; Hayes, G.B.; Feld, M.S.; Petras, R.E. Gastrointestinal tissue diagnosis by laser induced fluorescence spectroscopy at endoscopy. Gastrointest. Endosc. **1990**, *36*, 105–111.
14. Richards-Kortum, R.; Rava, R.P.; Petras, R.E.; Fitzmaurice, M.; Sivak, M.; Feld, M.S. Spectroscopic diagnosis of colonic dysplasia. Photochem. Photobiol. **1991**, *53*, 777–786.
15. Schomacker, K.T.; Frisoli, J.K.; Compton, C.C.; Flotte, T.J.; Richter, J.M.; Nishioka, N.S.; Deutsch, T.F. Ultraviolet laser-induced fluorescence of colonic tissue: Basic biology and diagnostic potential. Lasers Surg. Med. **1992**, *12*, 63–78.
16. Vo-Dinh, T.; Panjehpour, M.; Overholt, B.F.; Farris, C.; Buckley, F.P., III.; Sneed, R. In vivo cancer diagnosis of the esophagus using differential normalized fluorescence (DNF) indices. Lasers Surg. Med. **1995**, *16*, 41–47.
17. Andersson, P.S.; Montan, S.; Svanberg, S. Multispectral system for medical fluorescence imaging. IEEE J. Quantum Electron. **1987**, *23*, 1798–1805.
18. Tsurui, H.; Nishimura, H.; Hattori, S.; Hirose, S.; Okumura, K.; Shirai, T. Seven-color fluorescence imaging of tissue samples based on Fourier spectroscopy and singular value decomposition. J. Histochem. Cytochem. **2000**, *48* (5), 653–662.
19. Baert, L.; Berg, R.; van Damme, B.; D'Hallewin, M.-A.; Johansson, J.; Svanberg, K.; Svanberg, S. Clinical fluorescence diagnosis of human bladder-carcinoma following low-dose photofrin injection. Urology **1993**, *41*, 322–330.
20. Andersson-Engels, S.; Johansson, J.; Svanberg, K.; Svanberg, S. Laser-induced fluorescence in medical diagnostics. Proc. SPIE **1990**, *1203*, 76–96.

Marcel Dekker, Inc.
270 Madison Avenue, New York, New York 10016

21. Andersson-Engels, S.; Canti, G.; Cubeddu, R.; Eker, C.; afKlinteberg, C.; Pifferi, A.; Svanberg, K.; Svanberg, S.; Taroni, P.; Valentini, G.; Wang, I. Preliminary evaluation of two fluorescence imaging methods for the detection and the delineation of nasal cell carcinomas of the skin. Lasers Surg. Med. **2000**, *26*, 76–82.
22. Profio, A.E.; Doiron, D.R.; Balchum, O.J.; Huth, G.C. Fluorescence bronchoscopy for localization of carcinoma in situ. Med. Phys. **1983**, *10*, 35–39.
23. Alfano, R.R.; Tata, D.B.; Cordero, J.; Tomashefsky, P.; Longo, F.W.; Alfano, M.A. Laser induced fluorescence spectroscopy from native cancerous and normal tissue. IEEE J. Quantum Electron. **1984**, *20*, 1507–1511.
24. Tata, D.B.; Foresti, M.; Cordero, J.; Tomashefsky, P.; Alfano, M.A.; Alfano, R.R. Fluorescence polarization spectroscopy and time-resolved fluorescence kinetics of native cancerous, and normal rat kidney tissues. Biophys. J. **1986**, *50*, 463–469.
25. Alfano, R.R.; Lam, W.; Zarrabi, H.J.; Alfano, M.A.; Cordero, J.; Tata, D.B.; Swenberg, C.E. Human teeth with and without caries studied by laser scattering, fluorescence, and absorption spectroscopy. IEEE J. Quantum Electron. **1984**, *QE-20*, 1512–1515.
26. Vaarkamp, J.; ten Bosch, J.J.; Verdonshot, E.H. Light propagation through teeth containing simulated caries lesions. Phys. Med. Biol. **1995**, *40*, 1357–1387.
27. Schmitt, J.; Webber, R.L.; Walker, E.C. Optical determination of dental pulp vitality. IEEE Trans. Biomed. Eng. **1991**, *38*, 346–352.
28. Tang, G.C.; Oz, M.C.; Reid, V.; Steinglass, K.; Ginsberg, M.; Jacobowitz, L.; Alfano, R.R. Native fluorescence spectroscopy of thymus and fat tissues. Proc. SPIE **1993**, *1887*, 165–168.
29. Lam, S.; Hung, J.; Palcic, B. Detection of lung cancer by ratio fluorometry with and without photofrin II. Proc. SPIE **1990**, *1201*, 561–568.
30. Alfano, R.R.; Tang, G.C.; Pradhan, A.; Lam, W.; Choy, D.S.J.; Opher, E. Fluorescence spectra from cancerous and normal breast and lung tissues. IEEE J. Quantum Electron. **1987**, *QE-23*, 1806–1811.
31. Richards-Kortum, R., et al. Fluorescence Contour Mapping: Applications to Differentiation of Normal and Pathologic Human Tissues. In *1989 Conference on Lasers and Electro-Optics (Baltimore)*; April 1989.
32. Chung, Y.G.; Shwartz, J.; Gardner, C.; Sawaya, R.; Jacques, S.L. Fluorescence of normal and cancerous brain tissues: The excitation/emission matrix. Proc. SPIE **1995**, *2135*, 66–75.
33. Sterenborg, H.J.C.M.; Motamedi, M.; Wagner, R.F.; Duvic, M.; Thomsen, S.; Jacques, S.L. In vivo fluorescence spectroscopy and imaging of human skin tumors. Lasers Med. Sci. **1994**, *9*, 191–201.
34. Mahadevan, A., et al. Study of the fluorescence properties of normal and neoplastic human cervical tissue. Lasers Surg. Med. **1993**, *13*, 647.
35. Richards-Kortum, R.; Mitchell, M.F.; Ramanujam, N.; Mahadevan, A.; Thomsem, S. In vivo fluorescence spectroscopy: Potential for non-invasive automated diagnosis of cervical intraepithelial diagnosis of cervical intraepithelial neoplasia and use as a surrogate endpoint biomarker. J. Cell. Biochem., Suppl. **1994**, *19*, 111–119.
36. Heintzelman, D.L.; Utzinger, U.; Fuchs, H.; Zuluaga, A.; Gossage, K.; Gillenwater, A.M.; Jacob, R.; Kemp, B.; RichardsKortum, R.R. Optimal excitation wavelengths for in vivo detection of oral neoplasia using fluorescence spectroscopy. Photochem. Photobiol. **2000**, *72*, 103–113.
37. Werkhaven, J.A; Reinisch, L.; Sorrell, M.; Tribble, J.; Ossoff, R.H. Noninvasive optical diagnosis of bacteria causing otitis media. Laryngoscope **1994**, *104*, 264–268.
38. Warner, I.M., et al. Design considerations for a two-dimensional rapid scanning fluorometer. Anal. Chim. Acta **1979**, *109*, 361.
39. Warner, I.M., et al. Multidimensional luminescence measurements. Anal. Chem. **1985**, *57*, 463A.
40. Hung, J.; Lam, S.; LeRiche, J.; Palcic, B. Autofluorescence of normal and malignant bronchial tissue. Lasers Surg. Med. **1991**, *11*, 99–105.
41. Ramanujan, N.; Mitchell, M.F.; Mahadeevan, A.; Warren, S.; Thomsen, S.; Silva, E.; Richards-Kortum, R. In vivo diagnosis of cervical intraepithelial neoplasia using 337-nm-excited laser-induced fluorescence. Proc. Natl. Acad. Sci. U. S. A. **1994**, *91*, 10193–10197.
42. Ramanujam, N.; Mitchell, M.F.; Mahadevan, A.; Thomsen, S.; Silva, E.; Richards-Kortum, R. Fluorescence spectroscopy: A diagnostic tool for cervical intraepithelial neoplasia. Gynecol. Oncol. **1994**, *52*, 31–38.
43. Mitchell, M.F.; Cantor, S.B.; Ramanujam, N.; Tortolero-Luna, G.; Richards-Kortum, R. Fluorescence spectroscopy for diagnosis of squamous intraepithelial lesions of the cervix. Obstet. Gynecol. **1999**, *93*, 462–470.
44. Wang, T.D.; Crawford, J.M.; Feld, M.S.; Wang, Y.; Itzkan, I.; van Dam, J. In vivo identification of colonic dysplasia using fluorescence endoscopic imaging. Gastrointest. Endosc. **1999**, *49*, 447–455.
45. Kusonoki, Y.; Imamura, F.; Uda, H.; Mano, M.; Horai, T. Earl detection of lung cancer with laser-induced fluorescence endoscopy and spectrofluorometry. Chest **2000**, *118*, 1776–1782.
46. Lam, S.; MacAuley, C.; leRiche, J.C.; Palcic, B. Detection and localization of early lung cancer by fluorescence bronchoscopy. Cancer **2000**, *89*, 2468–2483.
47. Leffell, D.J.; Stetz, M.L. In vivo fluorescence of human skin. Arch. Dermatol. **1988**, *24*, 1518–1541.
48. Lohmann, W.; Nilles, M.; Bodeker, R.H. In situ differentiation between nevi and malignant melanomas by fluorescence measurements. Naturwissenschaften **1991**, *78*, 456–457.
49. Lohmann, W.; Paul, E. Native fluorescence of unstained cryo-section of the skin and melanomas and nevi. Naturwissenschaften **1989**, *76*, 424–426.
50. Lohmann, W.; Paul, E. In situ detection of melanomas by fluorescence measurements. Naturwissenschaften **1988**, *75*, 201–202.
51. Sterenborg, H.J.C.M.; Motamedi, M.; Wagner, R.F.; Thomsen, S.; Jacques, S.L. In vivo fluorescence spectro-

MARCEL DEKKER, INC.
270 Madison Avenue, New York, New York 10016

scopy for the diagnosis of skin diseases. Proc. SPIE **1994**, *2324*, 32–37.
52. Sterenborg, H.J.C.M.; Motamedi, M.; Wagner, R.F.; Duvic, M.; Thomsen, S.; Jacques, S.L. In vivo fluorescence spectroscopy and imaging of human skin tumours. Lasers Med. Sci. **1994**, *9*, 191–201.
53. Andersson-Engels, S.; Canti, G.; Cubeddu, R.; Eker, C.; afKlinteberg, C.; Pifferi, A.; Svanberg, K.; Svanberg, S.; Taroni, P.; Valentini, G.; Wang, I. Preliminary evaluation of two fluorescence imaging methods for the detection and the delineation of nasal cell carcinomas of the skin. Lasers Surg. Med. **2000**, *26*, 76–82.
54. Scott, M.A.; Hopper, C.; Sahota, A.; Springett, R.; McIlroy, B.W.; Bown, S.G.; MacRobert, A.J. Fluorescence photodiagnostics and photobleaching studies of cancerous lesions using ratio imaging and spectroscopic techniques. Lasers Med. Sci. **2000**, *15*, 63–72.
55. Blankenhorn, D.H.; Braunstein, H. Carotenoids in man: III. The microscopic patterns of fluorescence in atheromas, and its relation to their growth. J. Clin. Invest. **1956**, *35*, 160–165.
56. Sartori, M.; Sauebrey, R.; Kubodera, S.; Tittel, F.K.; Roberts, R.; Henry, P.D. Autofluorescence of atherosclerotic human arteries—a new technique in medical imaging. IEEE J. Quantum Electron. **1987**, *QE-23*, 1794–1797.
57. Kitrell, C.; Willet, R.L.; de las Santos-Pacheo, C.; Ratliff, N.B.; Kramer, J.R.; Malk, E.G.; Feld, M.S. Diagnosis of fibrous arterial atherosclerosis using fluorescence. Appl. Opt. **1985**, *24*, 2280–2281.
58. Richards-Kortum, R.; Mehta, A.; Hayes, G.; Cothren, R.; Kolubayev, T.; Kitrell, C.; Ratliff, N.B.; Kramer, J.R.; Feld, M.S. Spectral diagnosis of atherosclerosis using an optical fiber laser catheter. Am. Heart J. **1989**, *118*, 381–391.
59. Deckelbaum, L.I.; Stetz, M.L.; O'Brien, K.M.; Cutruzzola, F.W.; Gmitro, A.F.; Laifer, L.I.; Gindi, G.R. Fluorescence spectroscopy guidance of laser ablation of atherosclerotic plaque. Lasers Surg. Med. **1989**, *9*, 205–214.
60. Perk, M.; Flynn, G.J.; Smith, C.; Bathgate, B.; Tulip, J.; Yue, W.; Lucas, A. Laser-induced fluorescence emission: 1. The spectroscopic identification of fibrotic endocardium and myocardium. Lasers Surg. Med. **1991**, *11*, 523–534.
61. Perk, M.; Flynn, G.J.; Gulamhusen, S.; Yue, W.; Smith, C.; Barthgate, B.; Tulip, J.; Parfrey, N.A.; Lucas, A. Laser-induced fluorescence identification of sinoatrial and atriventricular nodal conduction tissue. Paging Clin. Electrophysiol. **1993**, *16*, 1701–1712.
62. Nassif, G.; Godard, B.; Fillette, F.; Lascault, G.; Grosgogeat, Y. The Use of Helium–Neon and Pulsed Dye Lasers in the Monitoring of the Heart Electrical Activity. Evolution to a Real Time Video Imaging of the Action Potential and Its Propagation on Myocardial Tissues. In *Proceedings of the International Conference on Lasers*; 1985; 44–50.
63. Dillon, S.; Morad, M. A new laser scanning system for measuring action potential propagation on the heart. Science **1981**, *214*, 453–456.
64. Docchio, F. Ocular fluorometry: Principles, fluorophores, instrumentation, and clinical applications. Lasers Surg. Med. **1989**, *9*, 515–532.
65. Zuclich, J.A.; Shimada, T.; Loree, T.R.; Bigio, I.J.; Strobl, K.; Nie, S. Lasers Life Sci. **1994**, *6*, 39–53.
66. Eppstien, J.; Bursell, S.-E. Non-invasive detection of diabetes mellitus. Proc. SPIE **1992**, *1641*, 217–226.
67. Piston, D.W.; Masters, B.R.; Webb, W.W. Three dimensionally resolved NAD(P)H cellular metabolic redox imaging of the in situ cornea with two-photon excitation laser scanning microscopy. J. Microsc. **1995**, *178*, 20–27.
68. Chance, B.; Williamson, J.R.; Jamieson, D.; Schoener, B. Properties and kinetics of reduced pyridine nucleotide fluorescence of the isolated and in vivo rat heart. Biochem. Z. **1965**, *341*, 367–377.
69. Renault, G.; Raynal, E.; Sinet, M.; Muffat-Joly, M.; Berthier, J.-P.; Cornillault, J.; Godard, B.; Pocidalo, J.-J. In situ double-beam NADH laser fluorimetry: Choice of a reference wavelength. Am. J. Physiol. **1984**, *246*, H491–H499.
70. Cordeiro, P.G.; Kirschner, R.E.; Hu, Q.Y.; Chiao, J.J.C.; Savage, H.; Alfano, R.R.; Hoffman, L.A.; Hidalgo, D.A. Ultraviolet excitation fluorescence spectroscopy: A non-invasive method for the measurement of redox changes in ischemic myocutaneous flaps. Plast. Reconstr. Surg. **1995**, *96*, 673–680.
71. Rampil, I.J.; Litt, L.; Mayevsky, A. Correlated, simultaneous, multiple-wavelength optical monitoring in vivo of localized cerebrocortical NADH and brain microvessel hemoglobin oxygen saturation. J. Clin. Monit. **1992**, *8*, 216–225.
72. Osbakken, M.; Mayevsky, A.; Ponomarenko, I.; Zange, D., et al. Combined in vivo fluorescence ad P-31 NMR to evaluate myocardial oxidative phosphorylation. J. Appl. Cardiol. **1989**, *4*, 305–313.
73. Beuthan, J.; Minet, O.; Muller, G. Observation of the fluorescence responses or the coenzyme NADH in biological samples. Opt. Lett. **1993**, *18*, 1098–1100.
74. Lohman, W., et al. Native fluorescence of the cervix uteri as a marker for dysplasia and invasive carcinoma. J. Obstet. Gynaecol. Reprod. Biol. **1989**, *31*, 249–253.
75. Andersson-Engels, S.; Johansson, J.; Svanberg, K.; Svanberg, S. Fluorescence imaging and point measurements of tissue: Applications to the demarcation of malignant tumors and atherosclerotic lesions from normal tissue. Photochem. Photobiol. **1990**, *51*.
76. Bottiroli, G., et al. Natural fluorescence of normal and neoplastic human colon: A comprehensive ex vivo study. Lasers Surg. Med. **1995**, *16*, 48–60.
77. Brookner, C.K.; Follen, M.; Bioko, I.; Galvan, J.; Thomsen, S.; Malpica, A.; Suzuki, S.; Lotan, R.; Richards-Kortum, R. Autofluorescence patterns in short-term cultures of normal cervical tissue. Photochem. Photobiol. **2000**, *71*, 730–736.
78. Boyer, J.; Mourant, J.R.; Bigio, I.J. Monte Carlo

Marcel Dekker, Inc.
270 Madison Avenue, New York, New York 10016

investigations of elastic scattering spectroscopy applied to latex spheres used as tissue phantoms. Proc. SPIE **1995**, *2389*, 103–112.
79. Bigio, I.J.; Mourant, J.R.; Boyer, J.; Johnson, T.; Shimada, T. Noninvasive identification of bladder-cancer with sub-surface backscattered light. Proc. SPIE **1994**, *2135*, 26–35.
80. Mourant, J.R.; Bigio, I.J.; Boyer, J.; Conn, R.L.; Johnson, T.; Shimada, T. Spectroscopic diagnosis of bladder cancer with elastic light scattering. Lasers Surg. Med. **1995**, *17*, 350–357.
81. Koenig, F.; Larne, R.; Enquist, H.; McGoven, F.J.; Schomacker, K.T.; Kollias, N.; Deutsch, T.F. Spectroscopic measurement of diffuse reflectance for enhanced detection of bladder carcinoma. Urology **1998**, *51*, 342–345.
82. Mourant, J.R.; Bigio, I.J.; Boyer, J.; Johnson, T.M.; Lacey, J.A. Elastic scattering spectroscopy as a diagnostic for differentiating pathologies in the gastrointestinal tract: Preliminary testing. J. Biomed. Opt. **1996**, *1*, 1–8.
83. Bigio, I.J.; Bown, S.G.; Kelly, C.; Lovat, L.; Pickarde, D.; Ripley, P.M. Developments in endoscopic technology for oesophageal cancer. J. R. Coll. Surg. Edinb. **2000**, 267–268.
84. Ge, Z.; Schomacker, K.T.; Nishioka, N.S. Identification of colonic dysplasia and neoplasia by diffuse reflectance spectroscopy and pattern recognition techniques. Appl. Spectrosc. **1998**, *52*, 833–839.
85. Zonios, G.; Perelman, L.T.; Backman, V.; Manahoran, R.; Fitzmaurice, M.; Van Dam, J.; Feld, M. Diffuse reflectance spectroscopy of human adenomatous colon polyps in vivo. Appl. Opt. **1999**, *38*, 6628–6637.
86. Wallace, M.B.; Perelman, L.T.; Backman, V.; Crawford, J.M.; Fitzmaurice, M.; Seiler, M.; Badizadigan, K.; Shields, S.J.; Itzkan, I.; Dasari, R.R.; Van Dam, J.; Feld, M.S. Endoscopic detection of dysplasia in patients with Barrett's esophagus using light-scattering spectroscopy. Gastroenterology **2000**, *119*, 677–682.
87. Sato, N.; Matsumura, T.; Shichiri, M.; Kamada, T.; Abe, H.; Hagihara, B. Hyperfusion, rate of oxygen consumption and redox levels of mitochondrial cytochrome $c(+c1)$ in liver in situ of anesthetized rat measured by reflectance spectrophotometry. Biochem. Biophys. Acta **1981**, *634*, 1–10.
88. Ono, K.; Kanda, M.; Hiramoto, J.; Yotsuya, K.; Sato, N. Fiber optic reflectance spectrophotometry for in vivo tissue diagnosis. Appl. Opt. **1991**, *30*, 98–105.
89. Anderson, R.R.; Parrish, J.A. The optics of human skin. J. Invest. Dermatol. **1981**, *77*, 13–19.
90. Saidi, I.S.; Jacques, S.L.; Tittel, F.K. Mie and Rayleigh modeling of visible-light scattering in neonatal skin. Appl. Opt. **1995**, *34*, 7410–7418.
91. Dawson, J.B.; Barker, D.J.; Ellis, D.J.; Grassam, E.; Cotteril, J.A.; Fisher, G.W.; Feather, J.W. A theoretical and experimental study of light absorption and scattering by in vivo skin. Phys. Med. Biol. **1980**, *25*, 696–709.
92. Feather, J.W.; Hajizadeh-Saffar, M.; Leslie, G.; Dawson, J.B. A portable scanning reflectance spectrophotometer using visible wavelengths for the rapid measurement of skin pigments. Phys. Med. Biol. **1989**, *34*, 807–820.
93. Hajizadeh-Saffar, M.; Feather, J.W.; Dawson, J.B. An investigation of factors affecting the accuracy of measurements of skin pigments by reflectance spectrophotometry. Phys. Med. Biol. **1990**, *35*, 1301–1315.
94. Kollias, N.; Baqer, A.H. Quantitative assessment of UV-induced pigmentation and erythema. Photodermatology **1988**, *5*, 53–60.
95. US patent #5,259,382.
96. Saidi, I.S.; Jacques, S.L.; Tittel, F.K. Preliminary Clinical Results of a Transcutaneous Reflectance Spectrophotometer for the Detection of Bilirubin in Neonates. In *Conference on Lasers and Electro-Optics*; OSA Technical Digest Series, 1994; Vol. 12, 150–151.
97. Marchesini, R.; Cascinelli, N.; Brambilla, M.; Clemente, C.; Mascheroni, L.; Pignoli, E.; Testori, A.; Ventroli, D.R. In vivo spectrophotometric evaluation of neoplastic and non-neoplastic skin pigmented lesions: II. Discriminant analysis between nevus and melanoma. Photochem. Photobiol. **1992**, *55*, 515–522.
98. Marchesini, R.; Tomatis, S.; Bartoli, C.; Bono, A.; Clemente, C.; Cupeta, C.; Del Prato, I.; Pignoli, E.; Sichirollo, A.E.; Cascinelli, N. In vivo spectrophotometric evaluation of neoplastic and non-neoplastic skin pigmented lesions: III. CCD camera-based reflectance imaging. Photochem. Photobiol. **1995**, *62*, 151–154.
99. Wallace, V.P.; Crawford, D.C.; Mortimer, P.S.; Ott, R.J.; Bamber, J.C. Spectrophotometric assessment of pigmented skin lesions: Methods and feature selection for evaluation of diagnostic performance. Phys. Med. Biol. **2000**, *45*, 735–751.
100. Bigio, I.J.; Bown, S.G.; Briggs, G.; Kelley, C.; Lakhani, S.; Pickard, D.; Ripley, P.M.; Rose, I.G.; Saunders, C. Diagnosis of breast cancer using elastic-scattering spectroscopy: Preliminary clinical results. J. Biomed. Opt. **2000**, *5* (2), 221–228.
101. Walls, J.; Knox, F.; Baildam, A.D.; Asbury, D.L.; Mansel, R.E.; Bundred, N.J. Can preoperative factors predict for residual malignancy after breast biopsy for invasive cancer? Ann. R. Coll. Surg. Engl. **1995**, *77*, 248–251.
102. Snider, H.; Dowlatshahi, K.; Fan, M.; Bridger, W.M.; Rayudu, G.; Oleske, D. Sentinel node biopsy in the staging of breast cancer. Am. J. Surg. **1998**, *176*, 305–310.
103. Johns, M.; Giller, C.; Liu, H. Computational and in-vivo investigation of optical reflectance from human brain to assist neurosurgery. J. Biomed. Opt. **1998**, *3*, 437–445.
104. Lin, W.C.; Toms, S.A.; Motamedi, M.; Jansen, E.D.; Mahadevan-Jansen, A. Brain tumor demarcation using optical spectroscopy: An in-vitro study. J. Biomed. Opt. **2000**, *5*, 214–220.
105. Hochheimer, B.F. Polarized light retinal photography of a monkey eye. Vis. Res. **1978**, *18*, 19–23.
106. Hielscher, A.H.; Mourant, J.R.; Bigio, I.J. Influence of particle size and concentration on the diffuse backscattering of polarized light from tissue phantoms and

biological cell suspensions. Appl. Opt. **1997**, *36*, 125–135.
107. Johnson, T.M.; Mourant, J.R. Polarized wavelength-dependent measurements of turbid media. Opt. Express **1999**, *4*, 200–216.
108. Pal, S.R.; Carswell, A.I. Polarization anisotropy in lidar multiple scattering from atmospheric clouds. Appl. Opt. **1985**, *24*, 3464–3471.
109. Dogariu, A.; Dogariu, M.; Richardson, K.; Jacobs, S.D.; Boreman, G.D. Polarization asymmetry in waves back-scattering from highly absorbance random media. Appl. Opt. **1997**, *36*, 8159–8167.
110. Dogariu, M.; Asakura. Polarization-dependent backscattering patterns from weakly scattering media. J. Opt. (Paris) **1993**, *24*, 271–278.
111. Rakovic, M.J.; Kattawar, G.W. Theoretical analysis of polarization patterns from incoherent backscattering of light. Appl. Opt. **1998**, *37*, 3333–3338.
112. Hielscher, A.H.; Eick, A.A.; Mourant, J.R.; Shen, D.; Freyer, J.P.; Bigio, I.J. Diffuse backscattering Mueller matrices of highly scattering medium. Opt. Express **1997**, *1*, 441–453.
113. Jacques, S.L.; Roman, J.R.; Lee, K. Imaging superficial tissue with polarized light. Lasers Surg. Med. **2000**, *26*, 119–129.
114. Muccini, J.A.; Kollias, N.; Phillips, S.B.; Anderson, R.R.; Sober, A.J.; Stiller, M.J.; Drake, L.A. Polarized-light photography in the evaluation of photoaging. J. Am. Acad. Dermatol. **1995**, *333*, 765.
115. Backman, V.; Gurjar, R.; Badizadegan, K.; Itzkan, I.; Dasari, R.R.; Perelman, T.; Feld, M.S. Polarized light scattering spectroscopy for quantitative measurement of epithelial structures in situ. IEEE J. Sel. Top. Quantum Electron. **1999**, *5*, 1019–1026.
116. Sokolov, K.; Drezek, R.; Gossage, K.; Richards-Kortum, R. Reflectance spectroscopy with polarized light: Is it sensitive to cellular and nuclear morphology. Opt. Express **1999**, *5*, 302–317.
117. Yao, G.; Wang, L.V. Propagation of polarized light in turbid media: Simulated animation sequences. Opt. Express **2000**, *7*, 198–203.
118. Vanitha, S.; Everett, M.J.; Maitland, D.J.; Walsh, J.T. Comparison of polarized-light propagation in biological tissue and phantoms. Opt. Lett. **1999**, *24*, 1044–1046.
119. Sankaran, V.; Walsh, J.T.; Maitland, C.J. Polarized light propagation through tissue phantoms containing densely packed scatterers. Opt. Lett. **2000**, *25*, 239–241.
120. Studinski, R.C.N.; Vitkin, I.A. Methodology for examining polarized light interactions with tissues and tissue-like media in the exact backscattering direction. **2000**, *5*, 330–337.
121. Cantor, C.R.; Shimmel, P.R. *Biophysical Chemistry: Part II. Techniques for the Study of Biological Structure and Function*; W.H. Freeman and Company: New York, 1980; 468–469.
122. Carey, P.R. *Biochemical Applications of Raman and Resonance Raman Spectroscopies*; Academic Press: New York, 1982; 97.
123. Parker, F.S. *Applications of Infrared, Raman, and Resonance Raman Spectroscopy in Biochemistry*; Plenum Press: 1984; Chap. 3.
124. Diem, M. *Introduction to Modern Vibrational Spectroscopy*; John Wiley and Sons: New York, 1993; 204–235, Chap. 8.
125. Mahadevan-Jansen, A.; Richards-Kortum, R. Raman spectroscopy for the detection of cancer and precancers. J. Biomed. Opt. **1996**, *1*, 31–70.
126. Le Gal, J.-M.; Manfait, M.; Theophanides, T. Applications of FTIR spectroscopy in structural studies of cells and bacteria. J. Mol. Struct. **1991**, *242*, 397–407.
127. Pouchert, C.J. *The Aldrich Library of FT-IR Spectra*, 1st Ed.; Aldrich Chemical Company, 1985; Vol. 1.
128. Chiriboga, L.; Yee, H.; Diem, M. Infrared spectroscopy of human cells and tissue: Part VI. A comparative study of histopathology and infrared microspectroscopy of normal cirrhotic and cancerous liver tissue. Appl. Spectrosc. **2000**, *54*, 1–8.
129. Mantsch, H.; Jackson, M. Molecular spectroscopy in biodiagnostics. J. Mol. Struct. **1995**, *347*, 187–206.
130. Floria, R.; Baumruk, V.; Srajbl, M.; Bednaova, L.; Stepanek, J. IR and Raman spectra, conformational flexibility, and scaled quantum mechanical force fields of sodium dimethyl phosphate and dimethyl phosphate anion. J. Phys. Chem. **1996**, *100*, 1559–1568.
131. Hubner, W.; Blume, A. Interactions at the lipid–water interface. Chem. Phys. Lipids **1998**, *96*, 99–123.
132. Hale, G.M.; Querry, M.V. Optical constants of water in the 200-nm to 200-μAppl. Opt. **1973**, *12*, 555–563.
133. Buschman, H.P.; Marple, E.T.; Wach, M.L.; Bennett, B.; Bakker Schut, T.C.; Bruining, H.A.; Bruschke, A.V.; van der Laarse, A.; Puppels, G.J. In vivo determination of the molecular composition of artery wall by intravascular Raman spectroscopy. Anal. Chem. **2000**, *72*, 3771–3775.
134. Shim, M.G.; Wong Kee Song, L.-M.; Marcon, N.E.; Wilson, B.C. In vivo near-infrared Raman spectroscopy: Demonstration of feasibility during clinical gastrointestinal endoscopy. Photochem. Photobiol. **2000**, *71*, 146–150.
135. Hanlon, E.B.; Manoharan, R.; Koo, T.-W.; Shafer, K.E.; Motz, J.T.; Fitzmaurice, M.; Kramer, J.R.; Itzkan, I.; Dasari, R.R.; Feld, M.S. Prospects for in vivo Raman spectroscopy. Phys. Med. Biol. **2000**, *45*, R1–R59.
136. Fung, M.F.K.; Senterman, M.; Eid, P.; Faught, W.; Mikhael, N.Z.; Wong, P.T.T. Comparison of Fourier-transform infrared spectroscopic screening of exfoliated cervical cells with standard Papanicolaou screening. Gynecol. Oncol. **1997**, *66*, 10–15.
137. Fung, M.F.K.; Senterman, M.K.; Mikhael, N.Z.; Lacelle, S.; Wong, P.T.T. Pressure-tuning Fourier transform infrared spectroscopic study of carcinogenesis in human endometrium. Biospectroscopy **1996**, *2*, 155–165.
138. Wong, P.T.T.; Lacelle, S.; Yazdi, H.M. Normal and malignant human colonic tissues investigated by pressure-tuning FT-IR spectroscopy. Appl. Spectrosc. **1993**, *47*, 1830–1836.
139. Malins, D.C.; Polissar, N.L.; Gunselman, S.J. Tumor

Marcel Dekker, Inc.
270 Madison Avenue, New York, New York 10016

progression to the metastatic state involves structural modifications in DNA markedly different from those associated with primary tumor formation. Proc. Natl. Acad. Sci. U.S.A. **1996**, *93*, 14047–14052.

140. Malins, D.C.; Polissar, N.L.; Schaefer, S.; Su, Y.Z.; Vinson, M.A. Unified theory of carcinogenesis based on order–disorder transitions in DNA-structure as studied in the human ovary and breast. Proc. Natl. Acad. Sci. U.S.A. **1998**, *95*, 7637–7642.
141. Benedetti, E.; Palatresi, M.P.; Vergamini, P.; Papineschi, F.; Andreucci, M.C.; Spremolla, G. Infrared characterization of nuclei isolated from normal and leukemic (B-CLL) lymphocytes: Part III. Appl. Spectrosc. **1999**, *40*, 39–43.
142. Benedetti, E.; Bramanti, E.; Papineschi, F.; Rossi, I.; Benedetti, E. Determination of the relative amount of nucleic acids and proteins in leukemic and normal lymphocytes by means of Fourier transform infrared micospectroscopy. **1997**, *51*, 792–797.
143. Benedetti, E.; Teodori, L.; Trinca, M.L.; Vergamini, P.; Salvati, F.; Mauro, F.; Spremolla, G. A new approach to the study of human solid tumor cells by means of FT-IR microspectroscopy. Appl. Spectrosc. **1990**, *44*, 1276–1280.
144. Haaland, D.M.; Jones, H.D.T.; Thomas, E.V. Multivariate classification of the infrared spectra of cell and tissue samples. Appl. Spectrosc. **1997**, *51*, 340–345.
145. Boydsron-White, S.; Gopen, T.; Houser, S.; Bargonetti, J.; Diem, M. Infrared spectroscopy of human tissue: V. Infrared spectroscopic studies of myeloid leukemia (ML-1) cells at different phases of the cell cycle. Biospectroscopy **1999**, *5*, 219–227.
146. Yazdi, Y.; Ramanujam, N.; Lotan, R.; Mitchell, M.F.; Hittelman, W.; Richards-Kortum, R. Resonance Raman spectroscopy at 257 nm excitation of normal and malignant cultured breast and cervical cells. Appl. Spectrosc. **1999**, *53*, 82–85.
147. Hawi, S.R.; Campbell, W.B.; Kajdacsy-Balla, A.; Murphy, R.; Adar, F.; Nithipatikon, K. Characterization of normal and malignant human hepatocytes by Raman microspectroscopy. Cancer Lett. **1996**, *110*, 35–40.
148. Manohoran, R.; Shafer, K.; Perelman, L.; Wu, J.; Chen, K.; Deinum, G.; Fitzmaurice, M.; Myles, J.; Crowe, J.; Dasari, R.R.; Feld, M.S. Raman spectroscopy and fluorescence photon migration for breast cancer diagnosis and imaging. Photochem. Photobiol. **1998**, *67*, 15–22.
149. Mahadeven-Jansen, A.; Folen, M.F.; Ramanujam, N.; Malpica, A.; Thomsen, S.; Utzinger, U.; Richards-Kortum, R. Near-infrared Raman spectroscopy for in vitro detection of cervical precancers. Photochem. Photobiol. **1998**, *68*, 123–132.
150. Romer, T.J.; Brennan, J.F.; Fitzmaurice, M.; Feldstein, M.L.; Deinum, G.; Myles, J.L.; Kramer, J.R.; Lees, R.S.; Feld, M.S. Histopathology of human coronary atherosclerosis by quantifying its chemical composition with Raman spectroscopy. Circulation **1998**, *97*, 878–885.
151. Romer, T.J.; Brennan, J.F.; Schut, T.C.B.; Wolthuis, R.; vanden Hoogen, R.C.M.; Emeis, J.J.; van der Laase, A.; Bruschke, A.V.G.; Puppels, G.J. Raman spectroscopy for quantifying cholesterol in intact coronary artery wall. Atherosclerosis **1998**, *141*, 117–124.
152. Weinmann, P.; Jouan, M.; Quy Dao, N.; Lacroix, B.; Groiselle, C.; Bonte, J.-P.; Luc, G. Quantitative analysis of cholesterol and cholestryl esters in human atherosclerotic plaques using near-infrared Raman spectroscopy. Atherosclerosis **1998**, *140*, 81–88.
153. Brooks, A.; Afanasyeve, N.I.; Makhine, V.; Bruch, R.F.; Kolyakov, S.F.; Artjushenko, S.; Butvina, L.N. New methods for investigations of normal human skin surfaces in vivo using fiber-optic evanescent wave Fourier transform infrared spectroscopy. Surf. Interface Sci. **1999**, *27*, 221–229.
154. Caspers, P.J.; Lucassen, G.W.; Wolthuis, R.; Bruining, H.A.; Puppels, G.J. In-vitro and in-vivo Raman-spectroscopy of human skin. Biospectroscopy **1998**, *4*, S31–S39.
155. Fender, S.; Schrader, B. Investigation of skin and skin lesions by NIR–FT–Raman spectroscopy. Fresenius J. Anal. Chem. **1998**, *360*, 609–613.
156. Caspers, P.J.; Lucassen, G.W.; Bruining, H.A.; Puppels, G.J. Automated depth-scanning confocal Raman microspectrometer for rapid in vivo determination of water concentration profiles in human skin. J. Raman Spectrosc. **2000**, *31*, 813–818.
157. Buschman, H.P.; Marple, E.T.; Wach, M.L.; Bennet, B.; Bakker Schut, T.C.; Bruining, H.A.; Bruschke, A.V.; van der Laarse, A.; Puppels, G.J. In vivo determination of the molecular composition of artery wall by intravascular Raman spectroscopy. Anal. Chem. **2000**, *72*, 3771–3775.
158. Qu, J.; MacAulay, C.; Lam, S.; Palcic, B. Laser-induced fluorescence spectroscopy at endoscopy: Tissue optics, Monte Carlo modeling, and in vivo measurements. Opt. Eng. **1995**, *34*, 3334–3343.
159. Mourant, J.R.; Hielscher, A.H. The Significance of Fiber Numerical Aperture for Optical Measurements of Turbid Media. In *OSA/TOPS Biomedical Optical Spectroscopy and Diagnostics*; 1996.
160. Bevilacqua, F.; Piguet, D.; Marquet, P.; Gross, J.D.; Tromberg, B.J.; Depeursinge, C. In vivo local determination of tissue optical properties: Applications to human brain. Appl. Opt. **1999**, *38*, 4939–4950.
161. Alexandrakis, G.; Farrell, T.J.; Patterson, M.S. Monte Carlo diffusion hybrid model for photo migration in a two-layer turbid medium in the frequency domain. Appl. Opt. **2000**, *39*, 2235–2244.